J|A|C|S
ARTICLES
Published on Web 00/00/0000

Interprotein Electron Transfer in a Confined Space: Uncoupling Protein Dynamics from Electron Transfer by Sol−Gel Encapsulation

Judith M. Nocek,[†] Shelby L. Hatch,[†] Jennifer L. Seifert,[†] Gregory W. Hunter,[‡] David D. Thomas,[‡] and Brian M. Hoffman*,[†]

Contribution from the Department of Chemistry, Northwestern University, Evanston, Illinois 60208, and Department of Biochemistry, Molecular Biology, & Biophysics, University of Minnesota, Minneapolis, Minnesota 55455

Received February 6, 2002

Abstract: In this paper, we describe the first observations of photoinitiated interprotein electron transfer (ET) within sol−gels. We have encapsulated three protein−protein complexes, specifically selected because they represent a full range of affinities, are sensitive to different types of dynamic processes, and thus are expected to respond differently to sol−gel encapsulation. The three systems are (i) the [Zn, Fe^{3+}L] mixed-metal hemoglobin hybrids, where the α_1-Zn and β_2-Fe subunits correspond to a "predocked" protein−protein complex with a crystallographically defined interface (Natan, M. J.; Baxter, W. W.; Kuila, D.; Gingrich, D. J.; Martin, G. S.; Hoffman, B. M. *Adv. Chem. Ser.* **1991**, *228* (*Electron-Transfer Inorg., Org., Biol. Syst.*), 201−213), (ii) the Zn−cytochrome *c* peroxidase complex with cytochrome *c*, [ZnC*c*P, Fe^{3+}C*c*], having an intermediate affinity between its partners (Nocek, J. M.; Zhou, J. S.; De Forest, S.; Priyadarshy, S.; Beratan, D. N.; Onuchic, J. N.; Hoffman, B. M. *Chem. Rev.* **1996**, *96*, 2459−2489), and (iii) the [Zn−deuteromyoglobin, ferricytochrome b_5] complex, [ZnDMb, $Fe^{3+}b_5$], which is loosely bound and highly dynamic (Liang, Z.-X.; Nocek, J.; Huang, K.; Hayes, R. T.; Kurnikov, I. V.; Beratan, D. N.; Hoffman, B. M. *J. Am. Chem. Soc.* **2002**, *124*, 6849−6859. Intersubunit ET within the hybrid does not involve second-order processes or subunit rearrangements, and thus is influenced only by perturbations of high-frequency motions coupled to ET. For the latter two complexes, sol−gel encapsulation eliminates second-order processes: protein partners encapsulated as a complex must stay together throughout a photoinitiated ET cycle, while proteins encapsulated alone cannot acquire a partner. It further modulates intracomplex motions of the two partners.

Dynamic processes of many kinds can influence electron transfer (ET), and other reactions, within protein−protein complexes. High-frequency fluctuations can modulate the redox energetics and/or reorganization energies of individual active sites,[1−6] or the interactions between sites.[7] A docked protein−protein complex can undergo "gated" interconversion[8] among reactive and nonreactive conformations; "mobile" complexes undergo true molecular diffusion that leads to second-order reactions between the partners. High-viscosity cryosolvent solutions have long been used to alter protein motions, including those coupled to interprotein ET (e.g., refs 9 and 10). Such studies, however, can be complicated because the cryosolvent medium can perturb the equilibrium binding constant of the complex, as well as second-order processes and the dynamics within the complex. Optically transparent rigid matrixes such as polyvinyl alcohol (PVA) and trehalose films are useful for modulating ligand-binding reactions[11−13] and for studying ET within "predocked" complexes,[5,14] but are not useful for studying reactions within dynamic protein−protein complexes. Here, we explore the possibility that encapsulating protein−protein complexes in the confined spaces of optically transparent sol−gels derived from tetramethyl orthosilicates (TMOSs)[15] might modulate interprotein ET through its influence on dynamic processes.

* Address correspondence to this author. E-mail: bmh@northwestern.edu.
[†] Department of Chemistry, Northwestern University.
[‡] Department of Biochemistry, University of Minnesota.

(1) Natan, M. J.; Baxter, W. W.; Kuila, D.; Gingrich, D. J.; Martin, G. S.; Hoffman, B. M. *Adv. Chem. Ser.* **1991**, *228* (*Electron-Transfer Inorg., Org., Biol. Syst.*), 201−213.
(2) Nocek, J. M.; Zhou, J. S.; De Forest, S.; Priyadarshy, S.; Beratan, D. N.; Onuchic, J. N.; Hoffman, B. M. *Chem. Rev.* **1996**, *96*, 2459−2489.
(3) Liang, Z.-X.; Nocek, M.; Huang, K.; Hayes, R. T.; Kurnikov, I. V.; Beratan, D. N.; Hoffman, B. M. *J. Am. Chem. Soc.* **2002**, *124*, 6849−6859.
(4) Marcus, R. A.; Sutin, N. *Biochim. Biophys. Acta* **1985**, *811*, 265−322.
(5) Dick, L. A.; Malfant, I.; Kuila, D.; Nebolsky, S.; Nocek, J. M.; Hoffman, B. M.; Ratner, M. A. *J. Am. Chem. Soc.* **1998**, *120*, 11401−11407.
(6) Hoffman, B. M.; Ratner, M. A. *Inorg. Chim. Acta* **1996**, *243*, 233−238.
(7) Daizadeh, I.; Medvedev, E. S.; Stuchebrukhov, A. A. *Proc. Natl. Acad. Sci. U.S.A.* **1997**, *94*, 3703−3708.
(8) Hoffman, B. M.; Ratner, M. R. *J. Am. Chem. Soc.* **1987**, *109*, 6237−6243.
(9) Nocek, J. M.; Stemp, E. D. A.; Finnegan, M. G.; Koshy, T. I.; Johnson, M. K.; Margoliash, E.; Mauk, A. G.; Smith, M.; Hoffman, B. M. *J. Am. Chem. Soc.* **1991**, *113*, 6822−6831.
(10) Zhou, J. S.; Kostic, N. M. *J. Am. Chem. Soc.* **1993**, *115*, 10796−10804.
(11) Gottfried, D. S.; Peterson, E. S.; Sheikh, A. G.; Wang, J.; Yang, M.; Friedman, J. M. *J. Phys. Chem.* **1996**, *100*, 12034−12042.
(12) Sastry, G. M.; Agmon, N. *Biochemistry* **1997**, *36*, 7097−7108.
(13) Dantsker, D.; Samuni, U.; Friedman, A. J.; Yang, M.; Ray, A.; Friedman, J. M. *J. Mol. Biol.* **2002**, *315*, 239−251.
(14) Ansari, A.; Berendzen, J.; Braunstein, D.; Cowen, B. R.; Frauenfelder, J.; Hong, M. K.; Iben, I. E. T.; Johnson, J. B.; Ormos, P.; Sauke, T. B.; Scholl, R.; Schulte, A.; Steinbach, P. J.; Vittitow, J.; Yound, R. D. *Biophys. Chem.* **1987**, *26*, 337.
(15) Brinker, C.; Scherer, G. *Sol-Gel Science: The Physics and Chemistry of Sol-Gel Processing*; Academic Press: New York, 1990.

10.1021/ja0258430 CCC: $22.00 © xxxx American Chemical Society

Sol−gel encapsulation of proteins has been applied to the study of ligand binding,[16,17] redox processes,[18]catalytic reactions,[19,20] and protein folding.[21] Of particular note to the present work, flash-photolysis studies of ligand binding to sol−gel-encapsulated hemoglobin (Hb) and myoglobin (Mb) have shown that one can uncouple conformational dynamics from heme ligation, and can isolate large populations of intermediate states that are otherwise inaccessible for study in solution, where conformational interconversions are rapid. For example, the results of time-resolved CO-rebinding measurements with HbCO demonstrated that sol−gel encapsulation restricts and even prevents the conformational interconversion that is linked to cooperative O_2 binding.[17,22,23] Such experiments suggest that sol−gel encapsulation might be used to modulate the dynamic processes linked with interprotein ET. Kostic and co-workers studied photoinduced redox reactions between encapsulated Zn-substituted cytochrome *c* (C*c*) and small oxidants,[18] but did not observe ET within protein−protein complexes in the gel phase.[24]

In this paper, we describe the first observations of photoinitiated interprotein ET within sol−gels. We have encapsulated three protein−protein complexes, specifically selected because they represent a full range of affinities, are sensitive to different types of dynamic processes, and thus are expected to respond differently to sol−gel encapsulation. The three systems are (i) the [Zn, Fe^{3+}L] mixed-metal Hb hybrids, where the α_1-Zn and β_2-Fe subunits correspond to a predocked protein−protein complex with a crystallographically defined interface,[1] (ii) the Zn−cytochrome *c* peroxidase complex with ferri-cytochrome *c*, [ZnC*c*P, Fe^{3+}C*c*], having an intermediate affinity between its partners,[2] and (iii) the [Zn−deuteromyoglobin, ferricytochrome b_5] complex, [ZnDMb, $Fe^{3+}b_5$], which is loosely bound and highly dynamic.[3] Intersubunit ET within the hybrid does not involve second-order processes or subunit rearrangements, and thus is expected to be influenced only by perturbations of high-frequency motions coupled to ET. For the latter two complexes, sol−gel encapsulation is expected to eliminate second-order processes: protein partners encapsulated as a complex must stay together throughout a photoinitiated ET cycle, while proteins encapsulated alone cannot acquire a partner. Encapsulation might also alter the kinetics of ET between docked partners by modifying the distribution of conformations and/or the kinetics of conformational interconversions within the complex. As we shall discuss, even the condition of confinement itself might modulate ET.

The optical and kinetic measurements reported here demonstrate that ET can be observed within all three complexes when they are encapsulated in a sol−gel. The sol−gel encapsulation indeed modulates the ET between partners in each of the three systems studied, and we suggest that the mechanism by which this occurs may be different in each case, consistent with their properties. However, measurements of triplet anisotropy decay show that the modulation does not reflect the obvious possibility of immobilization by the sol−gel, for each incorporated zinc protein is free to tumble on the ET time scale.

Experimental Procedures

Proteins. Hemoglobin (Hb) was isolated from human erythrocytes and purified by ion exchange chromatography as described previously.[25] The α(ZnP) chains and [α(ZnP), β(FeCO)] hemoglobin hybrid were prepared by the chain method of Yip[26] and purified by a procedure described for the [α(ZnP), β(FeCO)] hybrid.[25] The [α(ZnP), β(FeCO)] hybrid was oxidized with a 1.5-fold excess of $K_3Fe(CN)_6$ in 50 mM BisTrisCl at pH 6.0, and converted to its liganded adducts by washing the sample through a G-25 (fine) size exclusion column equilibrated with a 0.2 M solution of 1-methylimidazole, as described previously.[5] Zinc hemoglobin (ZnHb) was prepared with Zn−protoporphyrin IX[27] as described.[28] All buffers contained 50 μM inositol hexaphosphate (IHP).

Oxymyoglobin (Mb) was isolated from a bovine heart according to published procedures.[29,30] ApoMb and Zn−deuteroporphyrin-reconstituted Mb were prepared as described previously for sperm whale Mb.[31] Using the HPLC gradient elution procedure developed for sperm whale Mb, we find that the major component (∼75%) of the bovine Mb protein eluted from the cation exchange column (Beckman, SP5PW) during the first step of the gradient, much earlier than the sperm whale protein. The recombinant form of trypsin-solubilized ferricytochrome b_5 ($Fe^{3+}b_5$)[32] was used.

Recombinant MKT yeast cytochrome *c* peroxidase (C*c*P) was isolated and purified from *E. coli* according to published procedures.[33] Zinc-substituted C*c*P was prepared by heme extraction and reconstitution of C*c*P with zinc protoporphyrin IX (Frontier Scientific). Recombinant yeast iso-1-cytochrome *c* (C102T) (C*c*) was also isolated and purified from *E. coli* according to published procedures.[34]

Preparation of Solution Samples. Samples for solution-phase experiments were prepared in the dark under a nitrogen atmosphere and contained 2 mL of nitrogen-purged buffer, 10 mM D-glucose, 115 μg/mL glucose oxidase (Sigma, type X-S from *Aspergillus niger*), and 30 μg/mL thymol-free catalase from bovine liver (Sigma) to ensure anaerobicity.[35] Protein stock solutions were exchanged into 10 mM KPi buffer of the desired pH prior to the experiment using Centricon-10 microconcentrators (Millipore). For the complexes, an aliquot of a 0.2−1.0 mM stock solution of the Fe-containing partner protein was added to the Zn-substituted metalloprotein solution with a gastight syringe under a nitrogen blanket on a Schlenck line. Protein concentrations were determined spectrophotometrically using either a Hewlett-Packard diode array spectrophotometer (model 8451) or an Agilent Technologies spectrophotometer (model 8453): $\epsilon_{414\,nm}$(ZnDMb) = 364 mM^{-1} cm^{-1};[31] $\epsilon_{413\,nm}$($Fe^{3+}b_5$) = 117 mM^{-1} cm^{-1};[36] $\epsilon_{432\,nm}$(ZnC*c*P) = 196 mM^{-1} cm^{-1};[37] $\epsilon_{408\,nm}$(Fe^{3+}C*c*) = 106 mM^{-1} cm^{-1};[38] $\epsilon_{424\,nm}$([α(ZnP), β(FeCO)]) = 267 mM^{-1} cm^{-1}.[25]

(16) Shibayama, N.; Saigo, S. *J. Mol. Biol.* **1995**, *251*, 203−209.
(17) Khan, I.; Shannon, C. F.; Dantsker, D.; Friedman, A. J.; Perez-Gonzalez-de-Apodaca, J.; Friedman, J. M. *Biochemistry* **2000**, *39*, 16099−16109.
(18) Shen, C.; Kostic, N. M. *J. Am. Chem. Soc.* **1997**, *119*, 1304−1312.
(19) Ellerby, L.; Clinton, N. R.; Nishida, F.; Yamanaka, S. A.; Dunn, B.; Valentine, J. S.; Zink, J. I. *Science* **1992**, *225*, 1113−1115.
(20) Dave, B. C.; Dunn, B.; Valentine, J. S.; Zink, J. I. *Anal. Chem.* **1994**, *66*, 1120A−1127A.
(21) Eggers, D. K.; Valentine, J. S. *Protein Sci.* **2001**, *10*, 250−261.
(22) Das, T. K.; Khan, I.; Rousseau, D. L.; Friedman, J. M. *Biospectroscopy* **1999**, *5*, S64−S70.
(23) Shibayama, N.; Saigo, S. *J. Am. Chem. Soc.* **1999**, *121*, 444−445.
(24) Shen, C.; Kostic, N. M. *J. Electroanal. Chem.* **1997**, *438*, 61−65.
(25) Naito, N.; Huang, H.; Sturgess, W.; Nocek, J. M.; Hoffman, B. M. *J. Am. Chem. Soc.* **1998**, *120*, 11256−11262.
(26) Yip, Y. K.; Waks, M.; Beychok, S. *Proc. Natl. Acad. Sci. U.S.A.* **1977**, *74*, 64−68.
(27) Zn−mesoporphyrin IX−Hb was used in the luminescence anisotropy measurements.
(28) Zemel, H.; Hoffman, B. M. *J. Am. Chem. Soc.* **1981**, *103*, 1192−1201.
(29) Shimada, H.; Caughey, W. S. *J. Biol. Chem.* **1982**, *257*, 11893−11900.
(30) Wittenberg, J. B.; Wittenberg, B. A. *Methods Enzymol.* **1981**, *76*, 29−42.
(31) Nocek, J. M.; Sishta, B. P.; Cameron, J. C.; Mauk, A. G.; Hoffman, B. M. *J. Am. Chem. Soc.* **1997**, *119*, 2146−2155.
(32) Funk, W. D.; Lo, T. P.; Mauk, M. R.; Brayer, G. D.; MacGillivray, R. T. A.; Mauk, A. G. *Biochemistry* **1990**, *29*, 5500−5508.
(33) Ferrer, J. C.; Turano, P.; Banci, L.; Bertini, I.; Morris, I. K.; Smith, K. M.; Smith, M.; Mauk, A. G. *Biochemistry* **1994**, *33*, 7819−7829.
(34) Pollack, W. B. R.; Rosell, F. I.; Twitchett, M. B.; Dumont, M. E.; Mauk, A. G. *Biochemistry* **1998**, *37*, 6124−6131.
(35) Stankovich, M. T.; Schopfer, L. M.; Massey, V. *J. Biol. Chem.* **1978**, *253*, 4971−4979.
(36) Ozols, J.; Strittmatter, P. *J. Biol. Chem.* **1964**, *239*, 1018−1023.
(37) Stemp, E. D. A.; Hoffman, B. M. *Biochemistry* **1993**, *32*, 10848−10865.
(38) Margoliash, E.; Frohwirt, N. *Biochem. J.* **1959**, *71*, 570−572.

Preparation of Sol−Gel Samples. Proteins were encapsulated into tetramethyl orthosilicate (TMOS) sol−gels following the procedure of Ellerby et al.[19] We note that they prepared sols by sonicating a mixture containing TMOS (Aldrich), water, and HCl for ∼20 min, whereas we found that agitating the mixture for 30 s with a maxi-mix II (Thermolyne) vortex mixer produced equivalent results. In their preparation, they added a buffered stock solution of protein to a solution of sol plus added buffer; we added an aliquot of either an individual protein or a premixed protein−protein complex. The hydrolysis and condensation steps were performed at 4 °C, which decreases the rate of polymerization so as to allow adequate time for mixing, homogenization, and proportioning the sol−gel mixture into methacrylate semi-microcuvettes. To minimize shrinkage, a 1 mL layer of the same buffer was placed atop each gel, and the cuvette was capped. Gels were stored in the dark at 4 °C for a minimum of 12 h prior to any experiment, and all measurements with a gel were performed within 1 week of its preparation. Kinetic results were invariant over this period. The proteins were found to be stably encapsulated, and did not leach out into the capping buffer, even over periods far longer than gels were actually used.

Gels were allowed to polymerize in the presence of oxygen, but the kinetic measurements require deoxygenation. Because of the thickness of the sol−gels, it is tedious to deaerate gel samples by the techniques described by Shen and Kostic,[18] in which one directly purges the buffer phase with inert gas. Instead, we found that the enzymatic procedures employed for solution samples[31] could be adapted to deaerate sol−gel samples. In this method, aliquots of higher concentration stock solutions were added to give final concentrations of 115 μg/mL glucose oxidase (Sigma, type X-S from *A. niger*), 30 μg/mL catalase (Sigma, thymol-free form from bovine liver), and 10 mM glucose[35] in the nitrogen-purged buffer phase layered atop the sol−gel. Complete deaeration, determined by monitoring the oxygen quenching of the triplet state, was achieved within ∼3 h of incubation with enzymes.[39]

Measurements. The apparatus and technique for transient absorption spectroscopy were described previously.[31]

The apparatus used for collecting time-resolved phosphorescence anisotropy data was described by Ludescher and Thomas.[40] Decays were recorded using signal averaging from a single photomultiplier through polarizers alternating between vertical and horizontal orientations every 1000 pulses. The emission anisotropy, $r(t)$, is defined in eq 1,

$$r(t) = \frac{I_{vv}(t) - GI_{vh}(t)}{I_{vv}(t) + 2GI_{vh}(t)} \quad (1)$$

where $I_{vv}(t)$ and $I_{vh}(t)$ are the vertically and horizontally polarized components of the emission signal at time t. The value G is an instrumental correction factor, determined by examining a solution of erythrosin-labeled bovine serum albumin in 95% glycerol and adjusting to give zero residual anisotropy, the theoretical value for an isotropically tumbling chromophore. The anisotropy decay was fit to a sum of two exponentials, plus a constant (eq 2),[40] where r_0 is the initial anisotropy at time zero, ϕ_i is the rotational correlation time for component i, and A_∞ is the final anisotropy.

$$r_t/r_0 = \sum A_i e^{-t/\phi_i} + A_\infty \quad (2)$$

Frequency domain experiments were performed using a multifrequency cross-correlation phase and modulation fluorometer (ISS K2 with a tunable coherent Sabre Ar^+ laser (λ_{ex} = 514.5 nm)). Data were analyzed using Globals Unlimited software. The lowest modulation frequency on this instrument is 0.3 MHz, which is too high to determine ϕ_i for the sol−gel-encapsulated proteins. However, this approach could be used to determine r_0 when comparisons were made to glycogen as a scattering standard or Oregon Green as a fluorescence standard (τ = 4 ns).

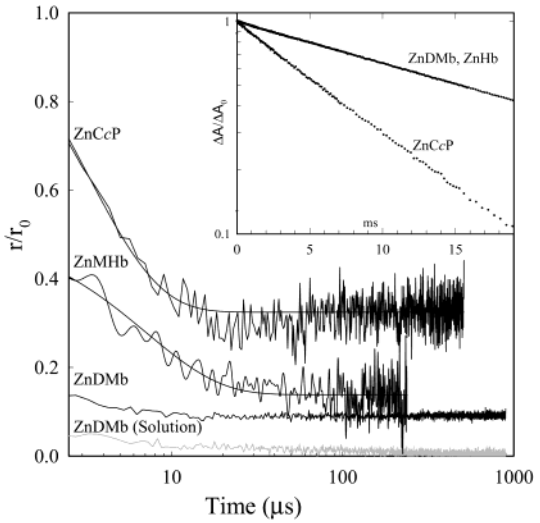

Figure 1. Triplet luminescence anisotropy decay traces of ZnC*c*P, ZnHb, and ZnDMb in sol−gel matrixes, and of ZnDMb in solution. Inset: Triplet decay traces of ZnDMb, ZnHb (Zn α-chains) (k_d = 50 s^{-1}) and ZnC*c*P (k_d = 100 s^{-1}) in sol−gel matrixes. Samples were prepared with 10 mM KPi at 20 °C, pH 6.0 for ZnDMb, pH 7.0 for ZnC*c*P and α(ZnP) chains, and pH 8.0 for ZnHb.

Results

Characterization of Encapsulated Proteins. We have encapsulated ZnHb and Zn α-chains as well as ZnC*c*P and ZnDMb, both with and without their respective ET partners ($Fe^{3+}b_5$ for ZnDMb and Fe^{3+}C*c* for ZnCcP). In each case, sol−gels with encapsulated protein(s) are homogeneous and optically transparent, with optical spectra that are indistinguishable from solution spectra of the protein(s) (data not shown). Several reports indicate that encapsulation *increases* protein thermal stability,[21,41] and indeed, all sol−gel samples studied were at least as stable as, or more stable than, samples at room temperature in ordinary fluid solution, and appeared to be indefinitely stable at 4 °C. Thus, not only can the basic proteins ZnDMb, ZnHb, and Fe^{3+}C*c* be encapsulated in the sol−gel matrix whose "walls" have a net negative charge, but so can the acidic proteins ZnC*c*P and $Fe^{3+}b_5$.[42]

The inset to Figure 1 shows the triplet-decay progress curves for ZnC*c*P, α(Zn)-chains, and ZnDMb encapsulated in deaerated sol−gels. The traces are monoexponential for at least 3 half-lives, and the triplet decay rate constants (k_d) are identical to the decay rate constants for the respective proteins in aqueous solution: ZnC*c*P, k_d = 100 s^{-1};[37] ZnDMb[31] α(Zn)-chains and ZnHb, k_d = 50 s^{-1}.[28] The solution and sol−gel samples all were photostable throughout any series of measurements reported. The fact that the triplet decay kinetics are not altered by encapsulation in the sol−gel confirms that sol−gel incorporation does not significantly perturb the proteins studied.

(39) We also found that glucose oxidase and catalase could be encapsulated along with the hemoproteins, and that these samples could be deaerated by addition of glucose to the buffer phase. The latter method is typically slow because it requires that glucose diffuse into the sol−gel phase.

(40) Ludescher, R. D.; Thomas, D. D. *Biochemistry* **1988**, *27*, 3343−3351.

(41) Das, T. K.; Khan, I.; Rousseau, D. L.; Friedman, J. M. *J. Am. Chem. Soc.* **1998**, *120*, 10268−10269.

(42) (a) We note that attempts to encapsulate the complex of C*c*P and C*c* were made previously, without any attempt to study ET, but apparently with less success. (b) Lin, C. T.; Catuara, C. M.; Erman, J. E.; Chen, K. C.; Huang, S. F.; Wang, W. J.; Wei, H. H. *J. Sol-Gel Sci. Technol.* **1996**, *7*, 19−26.

Triplet Anisotropy Measurements. The above experiments show that encapsulation occurs without disruption of the protein structure, but would not reveal nondisruptive interactions with the sol−gel matrix. Such interactions might slow the rotation of an encapsulated protein, or perhaps completely immobilize it through strong electrostatic binding or even covalent attachment to the silicate walls. To test for such effects, luminescence anisotropy decay measurements have been used to measure the rotational freedom of the encapsulated proteins.

Figure 1 shows time-resolved triplet anisotropy decay traces for ZnHb, ZnC*c*P, and ZnDMb in sol−gel matrixes, along with the corresponding trace for ZnDMb in aqueous solution. Prior studies with MgMb in solution show that it has a rotational correlation time of $\phi = 10.4$ ns.[44] As expected from this, the figure shows that most of the anisotropy of ZnDMb (17 kD) in aqueous solution is completely depolarized well within the deadtime of our instrument (<1 μs). When ZnDMb is encapsulated in a sol−gel, the major part of the luminescence anisotropy again depolarizes within <1 μs. This is consistent with the observation that rotation of sol−gel-encapsulated MgMb is impeded, but still occurs on a sub-microsecond time scale.[44]

In the sol−gel, the luminescence anisotropy for ZnDMb also displays a minor component that persists through the lifetime of the triplet signal (~0.9 ms), and thus is associated with protein that has been immobilized on that time scale. From knowledge of the initial anisotropy r_0 along with the residual anisotropy, one can calculate the fraction of immobilized ZnDMb in the sol−gel. To obtain (r_0), we measured the triplet anisotropy of ZnDMb dissolved in 95% glycerol at −10 °C; the high viscosity under these conditions slows the rotational diffusion to within the range measurable with our time-resolved apparatus. A fit of the resulting anisotropy decay to an exponential function yielded an initial anisotropy $r_0 = 0.28$ (and a rotational correlation time, $\phi = 6.5 \times 10^{-6}$ s). (For MgMb, $r_0 = 0.21$.)[43] The residual, persistent anisotropy for encapsulated ZnDMb of $r = 0.02$ then shows that ~6% of the ZnDMb in the sol−gel is immobilized through interactions with the silicate matrix, while the rest is free to tumble on a sub-microsecond time scale.

The anisotropy decays of the encapsulated ZnC*c*P (34 kD) and ZnHb (64 kD) also show two components (Figure 1). In each case, a major component decays with rotational times that are extended to more than 1 μs by interactions with the sol−gel matrix, while a minor component again comes from immobilized protein, whose luminescence anisotropy persists to the end of the data record (~1 ms). The anisotropy decay times for the rotationally mobile component are longer for ZnC*c*P and ZnHb than for ZnDMb, persisting to ~20 μs.[44]

In principle, the time course of the anisotropy decays for ZnC*c*P and ZnHb could be fit to determine r_0 for the two proteins, and, from this, the relative proportions of mobile and immobilized protein, along with the rotational correlation times for the mobile component. However, because most of the decay occurs within the instrumental deadtime, the fits to the data were not robust. In the case of ZnC*c*P, r_0 instead was obtained by two other, independent, methods. As with ZnDMb, r_0 was

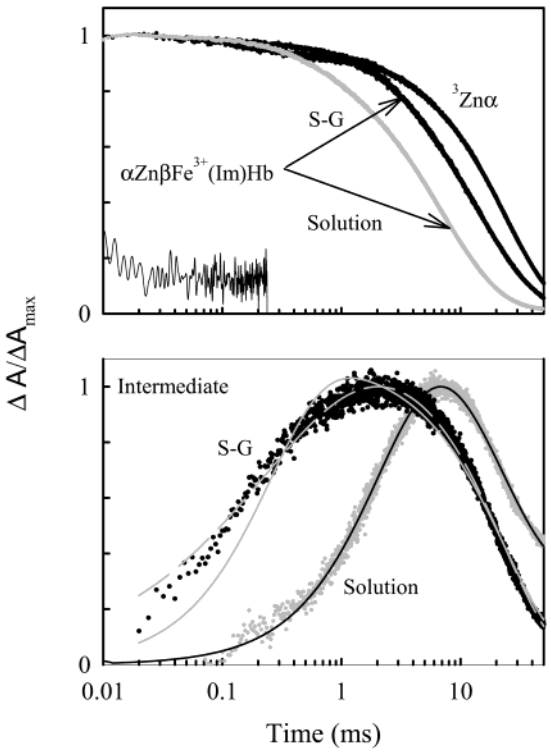

Figure 2. (Top**)** Triplet decays of α(ZnP) chains in solution and in sol−gel ($k_d = 50$ s^{-1}), and of [α(ZnP), β(Fe^{3+}Im)] Hb hybrids both in sol−gel ($k_{obs} = 70$ s^{-1}) and solution ($k_{obs} = 120$ s^{-1}). The anisotropy decay of ZnHb encapsulated in the sol−gel is included for comparison. **(**Bottom**)** Kinetic progress curves of the charge-separated intermediate **I** for [α(ZnP), β(Fe^{3+}Im)] Hb hybrids in solution and encapsulated in sol−gel. Solid lines are fits of both curves, respectively, to eq 5; the dashed line is a fit of the sol−gel data to eq 6. Conditions: 7 μM hybrid; 10 mM KPi buffer, pH 8.0, containing 200 mM 1-methylimidazole and 50 μM IHP; 20 °C.

obtained by measuring the time-resolved anisotropy decay for ^{3}ZnC*c*P in cold glycerol (95%, −10 °C), giving $r_0 = 0.10$; we also measured the frequency-domain fluorescence anisotropy of encapsulated ZnC*c*P and obtained the same r_0 ($r_0 = 0.11$). Thus, the residual anisotropy for ZnC*c*P in the sol−gel of approximately $r = 0.03$ indicates that ~70% of the incorporated ZnC*c*P is free, and ~30% is immobilized. Frequency-domain measurements for ZnHb in solution and encapsulated in sol−gel both yielded $r_0 = 0.24$: the residual anisotropy of $r = 0.04$ for the sol−gel sample thus indicates that ~85% of the encapsulated ZnHb is free and ~15% is immobilized.

Electron-Transfer Measurements. Substitution of the heme of one redox partner of a protein−protein ET pair with a closed-shell metalloporphyrin offers a means of studying the kinetics of the photoinitiated intracomplex ^{3}ZnP → Fe^{3+}P ET-quenching reaction (eq 3)

$$^3\text{ZnP} + \text{Fe}^{3+}\text{P} \rightarrow \text{ZnP}^+ + \text{Fe}^{2+}\text{P} \qquad (3)$$

and the subsequent intracomplex reaction whereby the charge-separated intermediate returns to the ground state by thermally activated ET from the Fe^{2+}P to the porphyrin-centered π-cation radical (ZnP$^+$) (eq 4).

$$\text{ZnP}^+ + \text{Fe}^{2+}\text{P} \rightarrow \text{ZnP} + \text{Fe}^{3+}\text{P} \qquad (4)$$

[α(ZnP), β(Fe^{3+}L)] Hb Hybrids. Flash photolysis was used to study the ET reactions within hybrids encapsulated in TMOS sol−gels (Figure 2). While the intrinsic triplet decay constant

(43) Gottfried, D. S.; Kagan, A.; Hoffman, B. M.; Friedman, J. M. *J. Phys. Chem.* **1999**, *103*, 2803−2807.
(44) Results for Hb are consistent with limits placed by an earlier spin-label study. Kar, L.; Johnson, M. E.; Bowman, M. K. *J. Magn. Res.* **1987**, *75*, 397−413.

of the Zn-substituted Hb chain, k_d, is not affected by encapsulation in a sol−gel (Figure 1), the triplet decay rate constant for the mixed-metal [α(ZnP), β(Fe^{3+}Im)] Hb hybrid which is increased due to ET quenching ($k_{obs} = k_d + k_{ET}$, where k_{ET} is the ET-quenching rate constant) is strongly affected by sol−gel encapsulation (Figure 2, top). In solution, the hybrid displays a triplet decay constant $k_{obs} = 120\ s^{-1}$, giving $k_{ET} = 70\ s^{-1}$, whereas in the sol−gel, the triplet decay constant for the encapsulated hybrid is measurably less, $k_{obs} = 70\ s^{-1}$, which corresponds to $k_{ET} = 20\ s^{-1}$. Such a decrease in k_{ET} also is observed when these Hb hybrids are embedded in PVA films.[5]

The observation of a transient-absorbance signal from the charge-separated ET intermediate [α($ZnP)^+$; β(Fe^{2+}L)] (**I**) confirms that triplet quenching within the hybrid results from ^{3}ZnP → Fe^{3+}P electron transfer. Figure 2 (bottom) shows the progress curves collected at the 436 nm triplet−ground, isosbestic for the ET intermediate in solution and in the TMOS sol−gel. This wavelength corresponds roughly to a maximum in the Fe^{2+}P/Fe^{3+}P difference spectrum, with the absorbance increase at this wavelength reflecting the formation of reduced heme. On the basis of our earlier work,[45] it was anticipated that the progress curves for **I** in solution would be described by eq 5

$$\Delta A = \frac{A_0(e^{-k_p t} - e^{-k_b t})}{k_b - k_p} \quad (5)$$

where k_b is the rate constant for the appearance of the ET intermediate and k_p is the rate constant for the decay of the triplet excited state. This function which describes the simple ET cycle of eqs 3 and 4 successfully describes the progress curves for the intermediate formed in solution and in PVA films.[5] In these cases, the intermediate appears more rapidly than the triplet decays, indicative that $k_b > k_p$. However, eq 5 does *not* adequately describe the curve for the ET intermediate in TMOS sol−gel (dashed line, Figure 2, bottom); as in solution, **I** for the hybrid in the sol−gel appears more rapidly than the triplet state decays, but its appearance is *not* well-described by a single-exponential rise (eq 5). Instead, the appearance of the intermediate signal, which corresponds to the ET return of **I** to ground, must be described with multiple rate constants. In the absence of a clearly defined kinetic model (and for convenience), we employed eq 6,

$$\Delta A = B[e^{-k_f t} - e^{(-k_r t)^n}] \quad (6)$$

which incorporates a "stretched exponential" function to model the rise of **I**. The fit to eq 6 shown in Figure 2 (bottom, solid line) gave as the rate parameter $k_r = 275\ s^{-1}$, and $n = 0.43$ as the distribution parameter; these correspond to quite a broad distribution of rates with an average of $k = nk_r = 118\ s^{-1}$, as compared to the well-defined value $k_b = 330\ s^{-1}$ [5] for the hybrid in solution. Indeed, the distribution likely is broader than the fit to the nonexponential rise might indicate, since **I** disappears exponentially, but with a rate constant less than that for triplet decay, $k_f < k_p$. This suggests that a subset of molecules is characterized by a value of k_b that is less than k_{obs}.

The [ZnC*c*P, Fe^{3+}C*c*] Complex. Figure 3 (top) shows normalized transient-absorbance decay curves for ^{3}ZnC*c*P and the [^{3}ZnC*c*P, Fe^{3+}C*c*] complex, each in solution and encapsulated in sol−gel. The measurements on encapsulated complexes were carried out with a large excess of Fe^{3+}C*c* (9:1) to ensure that the majority of the ZnC*c*P had bound Fe^{3+}C*c*. The solution sample had less Fe^{3+}C*c* (2:1) to minimize contributions from the second binding site on C*c*P, which complicates the ET kinetics.[37,46,47]

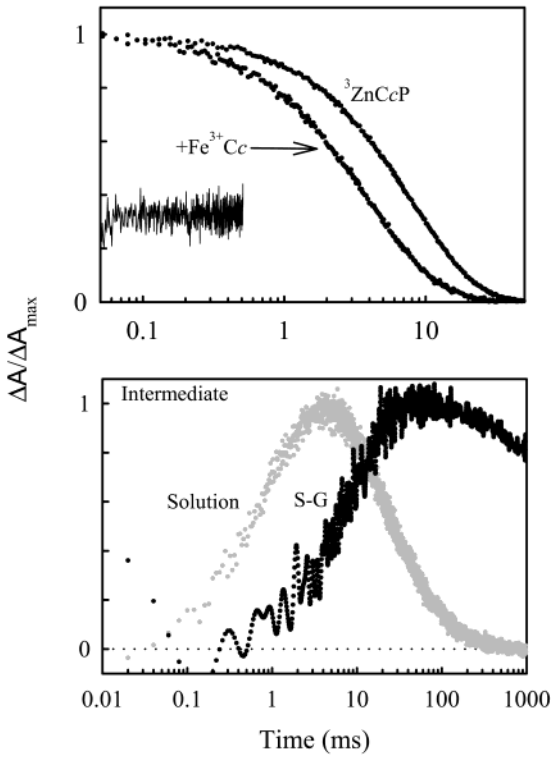

Figure 3. (Top**)** Triplet decays of ZnC*c*P in solution and sol−gel (k_d = 100 s^{-1}), and with the addition of excess Fe^{3+}C*c:* sol−gel (9:1); solution (2:1). The anisotropy decay of ZnC*c*P encapsulated in sol−gel is also shown for comparison. **(**Bottom**)** Kinetic progress curves for the charge-separated intermediate **I** for [ZnC*c*P, Fe^{3+}C*c*] in solution and encapsulated in sol−gel. Conditions: 10 mM KPi, pH 7.0; T = 20 °C.

The triplet state of ZnC*c*P is characterized by the intrinsic decay constant $k_d = 100\ s^{-1}$, in both solution and sol−gel. We reported earlier[37,46] that the kinetics for the complex of yeast C*c* with yeast C*c*P indicate that the free and bound components are in the slow-exchange kinetic limit; addition of substoichiometric amounts of Fe^{3+}C*c* to ZnC*c*P causes the triplet decay traces to become biexponential, with the slow phase corresponding to the uncomplexed ZnC*c*P ($k_{obs} = k_D = 100\ s^{-1}$), and the faster component corresponding to the decay of the triplet state in the complex ($k_{obs} = k_d + k_{ET}$). Consistent with our previous studies,[37,48] the decay trace for a solution of ZnC*c*P in the presence of 2 equivalents of Fe^{3+}C*c* (where nearly all of the ZnC*c*P resides within a complex) is monophasic (k_{obs} = 360 s^{-1}, which gives $k_{ET} = 260\ s^{-1}$) (Figure 3, top).

The decay profile for the [ZnC*c*P, Fe^{3+}C*c*] complex (1:9) encapsulated in a sol−gel also is described by a biexponential decay function, indicating the presence of two populations of ZnC*c*P. The slow phase, which accounts for ∼30% of the

(45) Natan, M. J.; Kuila, D.; Baxter, W. W.; King, B. C.; Hawkridge, F. M.; Hoffman, B. M. *J. Am. Chem. Soc.* **1990**, *112*, 4081−4082.

(46) Liang, N.; Kang, C. H.; Ho, P. S.; Margoliash, E.; Hoffman, B. M. *J. Am. Chem. Soc.* **1986**, *108*, 4665−4666.
(47) This will be addressed in future work.
(48) Ho, P. S.; Sutoris, C.; Liang, N.; Margoliash, E.; Hoffman, B. M. *J. Am. Chem. Soc.* **1985**, *107*, 1070−1071.

intensity, decays with the decay constant for free ZnC*c*P (k_d = 100 s^{-1}), despite the large excess (9:1) of Fe^{3+}C*c*. The fast phase accounts for ~70%, and its decay constant corresponds to that of the [^{3}ZnC*c*P, Fe^{3+}C*c*] complex in solution, k_{obs} = 350 s^{-1}.The percentage of ZnC*c*P incorporated as a complex is not changed by increasing the amount of Fe^{3+}C*c*. We interpret the above findings to indicate that the majority of ZnC*c*P (70%) is encapsulated in the sol−gel as an ET-active complex with Fe^{3+}C*c*, and that this complex exhibits ET quenching that is unchanged by encapsulation, with $k_{ET} = k_{obs} - k_d$ = 250 s^{-1}. The percentage of this form satisfactorily matches the percentage of ZnC*c*P that is free to tumble in the sol−gel. The minority form is assigned to the immobilized ZnC*c*P, which either fails to form a complex with Fe^{3+}C*c* or forms an ET-*inactive* one.[49]

The ET intermediate **I** formed when the active [ZnC*c*P, Fe^{3+}C*c*] complex undergoes photoinitiated ET according to eq 3 was monitored by transient-absorbance spectroscopy so as to characterize the thermal $Fe^{2+}P \rightarrow ZnP^+$ back electron transfer by which the charge-separated intermediate returns to the ground state. Figure 3 (bottom) shows the kinetic progress curves for the ET intermediate obtained at a ^{3}ZnP−ZnP isosbestic ($\lambda \approx$ 549 nm) for the solution and sol−gel [ZnC*c*P, Fe^{3+}C*c*] complexes. In solution, the signal for **I** exhibits multiphasic kinetics[50] appearing with a rate constant that is greater than the decay constant of the triplet and persisting long after the triplet signal has disappeared. This behavior has been attributed to the occurrence of intracomplex back ET within multiple, spectroscopically identical, conformations of the complex.[50] In the sol−gel, the signal for the ET intermediate also shows such multiphasic kinetics, but inspection of Figure 3 (bottom) shows that the rise of **I** is ca. 10-fold slower for the complex in the sol−gel than in solution, and its fall is at least 100-fold slower in the sol−gel.

The [ZnDMb, $Fe^{3+}b_5$] Complex. Figure 4 (top) shows the triplet decay traces for bovine ZnDMb in the presence of excess $Fe^{3+}b_5$ both in solution and in the sol−gel. In contrast to the much more tightly bound [ZnC*c*P, Fe^{3+}C*c*] complex, the [ZnDMb, $Fe^{3+}b_5$] complex in solution is in rapid exchange with its components.[31] As a result, the triplet decay curve can be described by an exponential function with a triplet decay rate constant (k_{obs}) that increases as a function of the concentration $Fe^{3+}b_5$; $k_{obs} = k_q + k_d$, where $k_q = k_2[Fe^{3+}b_5]$ and k_2 is the bimolecular quenching rate constant. In a solution where $[Fe^{3+}b_5] = 34\ \mu$M, the triplet decay constant for bovine ZnDMb, k_{obs} = 760 s^{-1}, corresponds to $k_2 = k_q/[Fe^{3+}b_5]$ = 21 μM^{-1} s^{-1}, which is 7-fold smaller than we reported for the complex with whale Mb[31] and 2-fold smaller than for horse Mb.[51]

On the basis of the results with the [ZnC*c*P, Fe^{3+}C*c*] complex, one might anticipate that trapping the [ZnDMb, $Fe^{3+}b_5$] complex in the gel would yield biphasic triplet decay traces, with the slow component associated with ZnDMb encapsulated by itself, and the rapid component with the encapsulated complex. However, the triplet decay trace for the sol−gel sample of ZnDMb in the presence of a 10-fold excess of $Fe^{3+}b_5$ is exponential, without measurable quenching: $k_{obs} \approx k_d$.

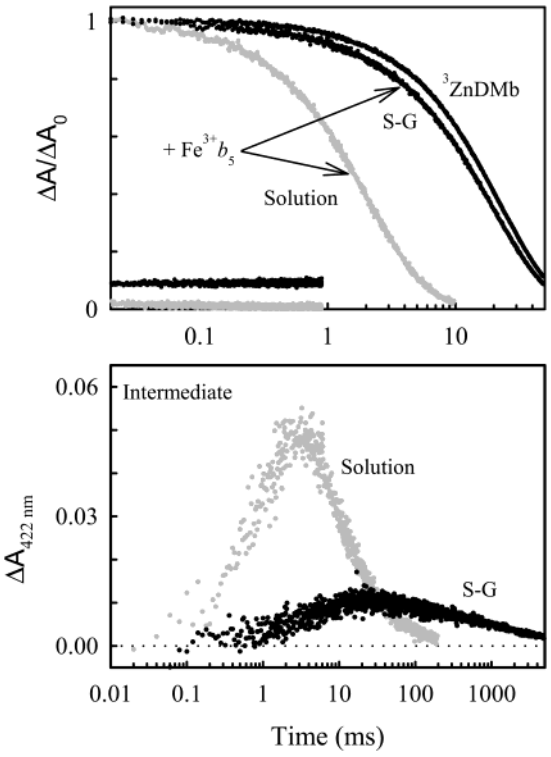

Figure 4. (Top) Triplet decays of ZnDMb in solution and sol−gel (k_d = 50 s^{-1}) and with the addition of excess $Fe^{3+}b_5$ in both sol−gel (k_{obs} = 50 s^{-1}) and solution (k_{obs} = 760 s^{-1}). The anisotropy decay of ZnDMb in solution and encapsulated in sol−gel is also shown for comparison. **(**Bottom**)** Kinetic progress curves for the charge-separated intermediate **I** for [ZnDMb, $Fe^{3+}b_5$] in solution and encapsulated in sol−gel. Conditions: in solution, ~5 μM ZnDMb and 34 μM $Fe^{3+}b_5$; in gel, 5.4 μM ZnDMb and 56.1 μM $Fe^{3+}b_5$; 10 mM KPi buffer, pH 6.0; 20 °C.

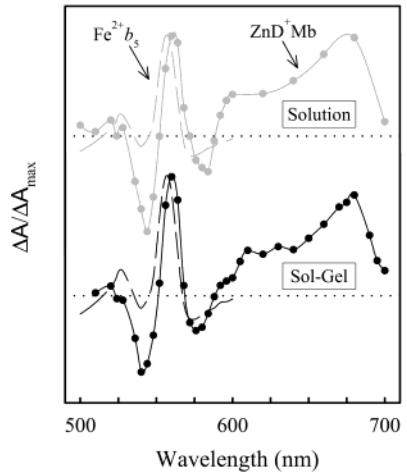

Figure 5. Kinetic difference spectra of **I** for [ZnDMb, $Fe^{3+}b_5$] in solution (50 ms after flash) and encapsulated in sol−gel (200 ms). Conditions: in solution, 3.2 μM ZnDMb and 15.1 μM $Fe^{3+}b_5$; in gel, 5.4 μM ZnDMb and 56.1 μM $Fe^{3+}b_5$; 10 mM KPi buffer, pH 6.0; 20 °C.

Despite the apparent lack of quenching in the sol−gel, we observe an absorbance transient from an ET intermediate after flash excitation of such samples (Figure 4, bottom). To prove that this signal is indeed associated with ET, transient difference spectra were collected for the complex in solution and in the sol−gel (Figure 5). These data show that the same kinetic difference spectra are obtained for the complex in solution and in the sol−gel; both spectra exhibit a maximum at 562 nm, resulting primarily from $Fe^{3+}b_5$ reduction (dashed line in Figure

(49) This is confirmed by data at other concentrations (not shown). The finding that the titrations in sol−gel mirror those in solution further shows that the proteins are encapsulated homogeneously throughout the gel.
(50) Wallin, S. A.; Stemp, E. D. A.; Everest, A. M.; Nocek, J. M.; Netzel, T. L.; Hoffman, B. M. *J. Am. Chem. Soc.* **1991**, *113*, 1842−1844.
(51) Liang, Z.-X.; Nocek, J. M.; Kurnikov, I. V.; Beratan, D. N.; Hoffman, B. M. *J. Am. Chem. Soc.* **2000**, *122*, 3552−3553.

5), and a maximum at 680 nm resulting from oxidation of ZnDMb to the porphyrin π-cation. This unambiguously establishes that, just as in solution, the transient signals from the sol−gel arise from the [ZnD$^+$Mb, Fe$^{2+}b_5$] ET intermediate. Thus, the [ZnDMb, Fe$^{3+}b_5$] complex is trapped in the sol−gel and is competent to undergo ET, even though this process is not revealed by the triplet quenching.

The observation of an intermediate despite the absence of measurable quenching can be understood in terms of the fact that Mb and Fe$^{3+}b_5$ exhibit "dynamic docking":[3,51,52] they bind weakly ($K_a \approx 10^3$ M^{-1}),[52] with no preferred structure, but instead can adopt a large ensemble of structures, the majority of which are inactive with regard to ET. The conditions for encapsulation (low ionic strength and pH 6) were chosen to optimize the yield of the complex. However, even under these conditions, less than 10% of the ZnDMb is likely to exist in a complex with Fe$^{3+}b_5$. Furthermore, if the docking conformations in the sol−gel faithfully reflect those in the solution, most docked conformations in the sol−gel will be unreactive. While the triplet decay is overwhelmingly dominated by the unreactive ZnMb, the ET intermediate signal only arises from ET-active complexes and is thus more readily observed because there is no "background" signal from the unreactive ZnMb.

Figure 4 (bottom) shows the time course for the intermediate associated with the complex in solution and in the sol−gel. Both signals persist long after the disappearance of the triplet state, up to ~0.1 ms in solution, but as with the [ZnC*c*P, Fe^{3+}C*c*] complex, both the appearance and subsequent disappearance of the signal in the sol−gel sample are much slower than in the solution sample.

Discussion

Kostic et al.[18] found that encapsulated ZnC*c* could be quenched by neutral molecules, such as oxygen, cationic quenchers, and anionic quenchers, but this occurred only when the quencher was added to the aqueous phase *after* gelation; no quenching was detected when macromolecule and quencher were encapsulated together, presumably because there was minimal incorporation as complex. In the present work, a combination of triplet-quenching, transient-absorption, and time-resolved triplet anisotropy measurements is used to demonstrate that three protein−protein complexes, exhibiting a broad range of binding affinities, have been encapsulated for study in a sol−gel matrix: a mixed-metal Hb hybrid, the [ZnC*c*P, Fe^{3+}C*c*(yeast)] complex, and the [ZnDMb, Fe$^{3+}b_5$] complex. In the case of the [Zn, Fe] Hb hybrid, this is not surprising given that the Zn and Fe partner chains are firmly linked within the Hb tetramer. However, the partners in the other two complexes are not so tightly linked: ZnC*c*P binds two molecules of C*c*, one with moderate affinity ($K_a \approx 10^7$ M^{-1}) and one with low affinity ($K_a \approx 10^3$ M^{-1}),[2] while Mb binds one cyt b_5 weakly, $K_a \approx 10^3$ M^{-1}.[3]

Numerous studies of sol−gel-encapsulated proteins show that their structures are not significantly perturbed by encapsulation, and that encapsulation, in fact, stabilizes proteins to denaturation.[17−19,21,22] Our optical and kinetic measurements indicate that the complexes we have encapsulated behave likewise. The triplet anisotropy measurements further show that the majority of each encapsulated Zn−metalloprotein is not immobilized by the sol−gel. The proteins tumble more slowly within the sol−gel environment than in solution, but rotate freely on a time scale of 20 μs or less. This suggests that a complex confined within a sol−gel "cell" is free to adopt an unconstrained active conformation on the ET time scale of 1−10 ms. The residual anisotropy in the traces indicates that a minority of each Zn protein is immobilized in the sol−gel, presumably by interactions with the silicate backbone. Interestingly, the acidic ZnC*c*P shows a mobility greater than that of the larger, basic ZnHb, so it appears that the rotational mobility of the proteins within the sol−gel is not primarily dependent on the net charge of the protein. Most importantly, as we now discuss, the kinetic experiments have demonstrated that sol−gel encapsulation can be used to modulate, and hence ultimately to understand, the linkage between dynamic motions and ET within protein−protein complexes. In this discussion, we summarize key aspects of the changes in ET kinetics caused by encapsulation and offer preliminary suggestions for possible mechanisms and further study.

Hb Hybrid. Sol−gel encapsulation of the [Zn, Fe] hybrid causes a modest decrease in the rate of photoinitiated ET, but has a much greater influence on the rate at which the ET intermediate returns to the ground state. In solution, this latter process is cleanly exponential, with a rate constant $k_b = 330$ s^{-1}, but this process becomes distributed upon encapsulation, with an average rate $k_b = nk_b = 118$ s^{-1}. In the sol−gel the majority signal has $k_b > k_p$, as in solution, but it appears that the process also has components with $k_b < k_p$. The observation of nonexponential kinetics for **I** in a "static" Hb tetramer demonstrates that encapsulation in a sol−gel indeed can be used to probe the coupling between high-frequency protein motions and the intratetramer, α_1–β_2 ET reaction, and enables their study!

The anisotropy-decay results show that the Hb hybrid is not bound to the sol−gel cell walls: the protein is free to tumble on a time scale far shorter than that of ET. Thus, it seems unlikely that interactions with the walls are responsible for the alterations in ET. This mobility also suggests that the alterations are not caused by modulation of the reorganization energy for ET, which we have shown[5,6] to exhibit an even more delicate control of ET than would appear from the standard ET theory.[4] Rather, we suggest that the confined space of a cell "passively" inhibits *high-frequency* fluctuations of the protein that are coupled to ET and which conceivably involve changes in the volume of the individual cells. An elegant heuristic model developed by Dill,[53] following the work of Minton,[54] shows that the free-energy cost for such fluctuations depends on the excess volume within the cell—the difference between the volume of the cell and volumes of the protein in its resting and fluctuated states. Thus, the observation of a distribution in rate constants could well reflect a distribution in cell volumes.

[ZnC*c*P, Fe^{3+}C*c*]. We find that ~70% of the encapsulated ZnC*c*P is rotationally mobile, that the same percentage of the encapsulated ZnC*c*P resides in an ET-reactive complex, and that these ratios do not change even when there is a large excess of Fe^{3+}C*c* present. We, therefore, identify the mobilized ZnC*c*P as being the ET-active protein. The optical spectra of the proteins in the complex are not altered by sol−gel encapsulation, so the

(52) Liang, Z.-X.; Jiang, M.; Ning, Q.; Hoffman, B. M. *J. Biol. Inorg. Chem.* **2002**, *7*, 580−588.
(53) Zhou, H.-X.; Dill, K. A. *Biochemistry* **2001**, *40*, 11289−11293.
(54) Minton, A. P. *Biophys. J.* **1992**, *63*, 1090−1100.

immobilized minority of the ZnC*c*P most likely binds to the walls without damage to the protein itself.

We have shown that ZnC*c*P binds C*c* at two distinct surface domains: a high-affinity domain with low reactivity for photoinitiated ET, and a low-affinity one with high reactivity.[2] Each of the ET-reactive C*c*Ps within the sol−gel necessarily has at least one C*c* encapsulated within the same cell, and the triplet state of the ET-active complex exhibits an exponential decay whose rate constant matches those of the 1:1 complex with Fe^{3+}C*c* in solution, within error. Nonetheless, the detection of a signal from the ET intermediate admits of the possibility that some of these ZnC*c*Ps are incorporated as the 2:1 complex, because we have shown[37] that the quenching at the high-affinity domain of the [ZnC*c*P, Fe^{3+}C*c*(yeast)] complex is attributable primarily to energy transfer, and that the photoinitiated ET primarily involves an Fe^{3+}C*c* bound at the second domain as part of a 2:1 complex.

Given this behavior, there are three possible explanations for the multiphasic kinetics of the ET intermediate **I** observed in the sol−gel and in solution. The simplest would be that the high-affinity domain is not completely ET inert, but rather that in solution the photoinitiated ET at this domain is overshadowed by ET at the other, more reactive, domain. If so, then the intermediate seen in the sol−gel could still be formed with Fe^{3+}C*c* bound at domain I, even if reaction at domain II is prevented by encapsulation of a 1:1 complex with Fe^{3+}C*c* bound at domain I. A second explanation would be that the Fe^{3+}C*c* of a 1:1 complex in a sol−gel cell is able to visit and react at domain II. The third possibility is that the intermediate being observed originates in a minority of 2:1 complex, but with the reaction at domain 2 resembling the "dynamic docking" reaction exhibited by Mb and cyt b_5. We defer discussion of this third option, and of possible experiments to distinguish among the three options, until we address the results for that complex. Regardless of the ultimate explanation, we see that sol−gel encapsulation has modulated interprotein ET by altering the relative motions of the two partners.

[ZnDMb, $Fe^{3+}b_5$]. Although we have not observed triplet quenching when ZnDMb is encapsulated with $Fe^{3+}b_5$, we have, nonetheless, observed the transient absorbance spectrum of the intermediate formed by photoinitiated intracomplex ET. Both the appearance and disappearance of the signal of the ET intermediate are slowed by sol−gel incorporation. A possible explanation for these observations is suggested by our recent studies of this complex in solution. The [ZnDMb, $Fe^{3+}b_5$] complex exhibits a new dynamic docking paradigm for protein−protein interaction: Mb binds b_5 in numerous conformations over a broad area of its surface, but reaction occurs only in a minority of weakly bound, but highly reactive, conformations.[3,51,52] In the context of this paradigm, the slowed kinetics in the sol−gel may be indicating that encapsulation restricts the conformational mobility of the trapped complex, decreasing the probability that it achieves its optimal orientation for ET. This could occur even though the anisotropy measurements indicate that the ZnDMb in the sol−gel matrix rotates freely on the ET time scales.

As noted above, a dynamic docking picture may also apply to the reaction at the low-affinity domain of ZnC*c*P, which according to this picture, would have high reactivity at select, weakly bound conformations. The "second" weakly bound Fe^{3+}C*c* in an encapsulated ternary [ZnC*c*P, Fe^{3+}C*c*] complex would react much as does a weakly bound $Fe^{3+}b_5$ encapsulated with ZnMb. Thus, it might give little contribution to quenching, yet be the source of the observed ET intermediate. We can test this possibility, as we did for the complex in solution,[37] by examining the intensity of the signal from **I** as a function of the concentration of Fe^{3+}C*c*. The intensity of the **I** signal will increase with [Fe^{3+}C*c*] past the 1:1 point if the signal comes from the ternary complex, whereas it will be independent of [Fe^{3+}C*c*] past this point if it comes from the binary complex.

Most importantly, the absence of significant triplet quenching in the [ZnDMb, $Fe^{3+}b_5$] complex indicates that sol−gel encapsulation has effectively eliminated second-order processes; proteins encapsulated as a complex stay together, and those encapsulated alone cannot acquire a partner.

Summary. We have observed intracomplex ET in three different types of protein−protein complexes encapsulated in TMOS sol−gels. In all three instances the ET kinetics are modified by the sol−gel encapsulation, but it is likely that different dynamic processes are associated with the observed ET reaction in each of these complexes. This study represents the initial step in using sol−gel encapsulation as a tool for temporally isolating the different dynamic processes coupled to ET in protein−protein complexes.

Acknowledgment. This work has been supported by the NIH (Grant HL 63202, B.M.H.; Grant GM 27906, D.D.T.).

JA0258430